ISTITUTO NAZIONALE DI FISICA NUCLEARE

Laboratorio Nazionale del Sud

INFN/TC-95/12
3 Marzo 1995

D. Rifuggiato, L. Calabretta:

STUDY AND OPERATION OF THE INJECTION, ACCELERATION AND EXTRACTION PROCESSES FOR THE LNS SUPERCONDUCTING CYCLOTRON COMMISSIONING

PACS: 29.20.HM, 29.27.-a, 29.27.ac

SIS-Pubblicazioni
dei Laboratori Nazionali di Frascati

INFN - Istituto Nazionale di Fisica Nucleare
Laboratorio Nazionale del Sud

INFN/TC-95/12
3 Marzo 1995

STUDY AND OPERATION OF THE INJECTION, ACCELERATION AND EXTRACTION PROCESSES FOR THE LNS SUPERCONDUCTING CYCLOTRON COMMISSIONING

D. Rifuggiato, L. Calabretta

INFN–Laboratorio Nazionale del Sud, Via S. Sofia 44, I–95123 Catania, Italy

1. Introduction

The LNS Superconducting Cyclotron is a three sectors, K=800, K_{foc}=200 compact machine, which is being operated as a booster of a 15 MV Tandem. All of the features of this machine have been extensively presented in [1]. For the LNS Cyclotron commissioning, a ^{58}Ni beam has been chosen to be accelerated to 30 MeV/a.m.u.. The reasons for this choice are both the interest of nuclear physicists in doing experiments with this beam, and the position of this ion in the operating diagram of the machine, well far from the boundaries, which in principle means that limiting values of the parameters are not required. Here we report the injection, acceleration and extraction studies that have been accomplished in order to find out the nominal values of the machine parameters for this ion. Part of this study has been suggested by operational features occurred while doing the beam tests and can therefore be considered as an effort to explain them.

Since it will very often be mentioned henceforth, it is worthwhile to give a short description of the main diagnostics tool of the machine: it is a probe moving in the center of a hill along the corresponding spiral. This probe had been originally designed as a current probe, but, based on the experience gained [2] by operating with a different diagnostic tool, namely the alumina + TV camera complex, it was decided to replace the current read-out system with this new system. It is also planned to install [3] a particular head which allows to choose the working mode of the probe between the current read-out and the beam visualization.

2. Injection study

The ^{58}Ni beam, accelerated by the Tandem, is radially injected [4] into the Cyclotron, after having gone through a beam line [5] made up of three 60° dipoles and fourteen quadrupoles, ending with a steering magnet able to change the direction of the beam by a few degrees. As clearly shown in fig. 1, the beam spends in a valley most of its injection path inside the pole of the cyclotron, then reaches a stripper foil placed in the following hill.

The only data assumed for the injection study are the final energy (E_f) at the cyclotron exit and the ion type. The charge state of the injected ion (Q_i) and of the accelerated ion (Q_f), the energy of the injected ion (E_i) are to be chosen. The choice of these parameters was based on:

- the evaluation of the charge state distributions after the gaseous stripper of the Tandem and especially after the foil stripper of the Cyclotron [6];
- the magnetic field value in the center of the machine;
- the constraints imposed to the injection trajectory by the geometrical limits of the injection channel and by the position range of the stripper system [7].

From the first two conditions the couple Q_i=4, Q_f=16 was selected together with a Tandem voltage of about 10 MV; the verification of the injectability of this beam (the third item) slightly changed the Tandem voltage to 9.5 MV.

The injection calculations were accomplished with a 120° symmetric magnetic field map [8] generated by taking account of the recent magnetic measurements [9], extended up to the radius of the steering magnet (r = 2500 mm). A description of the study procedure is here reported. The equilibrium orbit corresponding to E_i diminished by the energy loss due to the stripper crossing, is calculated with azimuthal steps of 0.1°, in order to be matched with the injection trajectory at the stripper position. An automatic procedure reads the equilibrium orbit data and allows to find out the injection trajectory, which must not hit the injection channel and must go through the center of the steering magnet. For the beam chosen, the stripper position resulting from this procedure is quite reachable with the positioning system. A parameter determined by this procedure is the field of the steering magnet.

In order to realize a very good matching between the Tandem beam emittance and the acceptance of the Cyclotron, the beam behaviour was studied in the horizontal and vertical phase spaces. The radial and axial eigenellipses at the stripper position were calculated assuming an emittance value of 4.8π mm·mrad, which is about four times larger than the estimated one [10]. Then, following the same

walk-back procedure used for the calculation of the injection trajectory, eight particles belonging to the eigenellipse were transported to the steering magnet at the entrance of the machine, so as to obtain the beam configuration and the radial and axial envelope of the beam along the injection trajectory (figs. 2,3). In particular, the beam parameters at the steering magnet position (beam ellipse parameters, linear and angular dispersion R_{16} and R_{26}) are used to tune the matching section of the coupling beam line between the Tandem and the Cyclotron.
A list of the injection parameters is displayed in tab. 1.

3. Injection operation

In the very first phase of the commissioning, a TV camera was placed in one of the yoke penetrations designed for the second electrostatic deflector (E2), see fig. 1, pointing towards an alumina plate positioned at the same azimuth as the stripper, and shifted towards the centre of the machine. With this tool it was possible to see the beam spot in a position very close to the stripper. With the deflector E2 installed, this system was of course given up. Then we decided to use the moving probe to see the beam, not stripped, clearing the stripper at its inner or outer (referred to the center of the machine) sides. In fact the radial position of the beam at the stripper azimuth can be varied by properly adjusting the steering magnet position: a 0.5° variation at the entrance of the machine causes a 2.5 cm variation of the radial position at the stripper azimuth. Once the beam is not stripped, the trajectory beyond the stripper position is quite different from the accelerated orbit, and the radial position of the beam spot on the probe is by far out of the stripping radius (fig. 4).
In order to locate the radial position of the moving probe, a simulation has been accomplished, consisting in varying the bending angle with respect to the injection trajectory by properly adjusting the steering magnet. This simulation shows that the radial position of the trajectory on the moving probe (at the center of the hill following the stripper hill) is not much sensitive on the bending angle of the steering magnet and consequently on the radial position of the trajectory at the stripper azimuth. This helps a lot in looking for the beam spot on the alumina plate. It was also experimentally realized, and then verified by simulation, that a focus condition at the moving probe position does not imply a similar beam condition at the stripper position. Then a correct tuning of the quadrupoles of the matching section can be done only by looking at the stripped beam shape,

which has been achieved by placing the moving probe at the same radius as the stripper radius, so as to look at the stripped beam about 120° after the stripper position.

4. Acceleration study

First of all, the equilibrium orbit properties have been studied by means of a code [11] giving information on the radial positions where the resonances occur and on the phase trend of the accelerated ion for a certain dee voltage value. The resonances $\nu_r = 1$ and $\nu_r = 2\nu_z$ are located at r_{av} ~82.6 cm and r_{av} ~82.4 cm respectively, while the resonance $\nu_r + 2\nu_z = 3$, particularly dangerous for the beam stability, is not at all crossed.

In order to study the accelerated beam properties and find out the parameters of the beam to be extracted, the Spiral Gap code [12] has been used to simulate the path of the beam during acceleration; as a starting point for acceleration, an equilibrium orbit (e.o.) has been chosen where the phase is close to 0°, namely the e.o. corresponding to E = 18 MeV/a.m.u. The dee voltage was assumed to be 50 kV, regarded as a "safe" value for a commissioning operation. The field map used is a 360° one, obtained from the 120° symmetric one, adding the measured significant imperfection harmonics contribution and the imperfection harmonics of the trim coils. Moreover, this map takes account of the contribution of the magnetic channels and compensating bars (see forth) and is therefore a result of successive iterations: at first, a certain configuration of channels and bars was considered. After two extraction runs, the final configuration was found out.

A set of twenty room temperature coils (trim coils) is available to get the right field shape for each ion to be accelerated. They all are three-fold symmetric, consisting of three identical windings around the hills; for most of them one power supply feeds one trim coil, while for the last two ones, n. 19, 20 and for n. 3, 4, each winding on a hill is fed independently, allowing to provide a controlled I harmonic contribution. A particular study was done in order to find out the I harmonic contribution that the last two harmonic coils have to provide to separate as much as possible the last two orbits before extraction, preserving at the same time the beam quality; the beam behaviour in the phase space was investigated so as to find out the I harmonic amplitude and phase (fig. 5). In tab. 2 the acceleration parameters are listed.

5. Acceleration operation

For these beam tests, the alumina head of the moving probe was equipped with an aluminium strip, 2 mm wide, to read the beam current too. In the first tests, a remarkable beam loss (about 90%) occurred in the final radial range, 3 centimeters before extraction. The reason for this loss was immediately investigated. A strong suggestion came from having detected radioactivity in the gap between one hill and the following valley, above and below the median plane, in a radial position approximately corresponding to r=83 cm.

So the reason for the intensity loss was guessed to be an axial blow-up of the beam, caused when crossing the resonance $\nu_r = 2\nu_z$, which couples the radial and the axial motion. Therefore, this phenomenon should be due to radial oscillations occurring during acceleration and, in particular, when crossing the resonance. This means that the beam is off-centered in comparison to the accelerated equilibrium orbit, which can happen either at the beginning of acceleration, due to a wrong injection procedure, or during acceleration, due to electric and magnetic field imperfections [13].

A set of simulations was done in order to ascertain the off-centering effect on the axial width of the beam. Assuming the equilibrium orbit at injection as a starting point, the orbit was centered by a I harmonic bump coming from the harmonic coils 3 and 4. The axial size of the beam (z_{max}) was found out by simulating the acceleration of the central ray and of eight particles belonging to the axial eigenellipse contour; the supposed emittance value was 4.8π mm·mrad at the injection energy. Data were acquired every 10° in order to find out the beam size for each turn. As a reference case we considered the result of this procedure with the orbit centered. Then the procedure described was applied to an off-centered orbit with Δr=5 mm, Δp_r=0. The acceleration figure in the (x,p_x) plane, with $x = r - r_{e.o.}$ and $p_x = p_r - p_{r_{e.o.}}$, is shown in fig. 6. Two more cases were considered, belonging to the contour of the previous figure: Δr=0, Δp_r=4 mm and Δr=3 mm, Δp_r=3 mm. As shown in fig. 7, for all the three cases z_{max} is increasing by the same amount, i.e. ~2.5 mm, which qualitatively confirms the origin of the axial blow-up, namely the radial-axial motion coupling.

A few simulations were performed in order to find out the dependance of z_{max} on the off-centering extent, which resulted to be quadratic up to Δr=6 mm (and Δp_r=0), while for Δr greater than 6 mm the beam totally blows up axially.

Moreover, the application of the extraction bump by the last two harmonic coils, which gives a good inter-turn separation, through the controlled excitation of the

ν_r=1 resonance, also makes the axial beam size increase. In fig. 8 this effect is shown for a beam off-centered by 2 mm, in comparison with a centered beam which feels the effect of the I harmonic bump and with the former off-centered beam without the application of the I harmonic bump. This is due to the close location of the two resonances, which are crossed in a range of two millimeters. Last, it was verified that there is a weak dependance, namely a square root dependance, on the emittance value of the beam.

6. Extraction study and operation

The extraction system [14] consists of two electrostatic deflectors, E1 and E2, spanning an azimuthal range of 52 and 40 degrees respectively, followed by 8 passive magnetic channels, one of which is positioned inside the yoke (fig. 1). Two iron bars (C1,C2) are used to compensate the I harmonic perturbation produced by the channels. The extraction study shows that 5 (of 7) magnetic channels are enough to focus the beam along the extraction path and that the two electrostatic deflectors, positioned according to the extraction trajectory, have to provide an electric field (supposed to be the same for both of them) of 74.398 kV/cm, which corresponds to a voltage of 59.52 kV for the present 8 mm gap. The beam envelope along the extraction path is shown in fig. 9. The extraction parameters are displayed in tab. 3.

A big effort [15] was done to install a diagnostic tool at the entrance of the second deflector, so as to make easier the extraction operation. After the second deflector, the first available diagnostic tool is a differential current probe placed in front of the magnetic channel M2 (fig. 1). The diagnostics equipment assembled on E2 consists of an alumina plate whose outer (referred to the machine center) edge coincides with the inner edge of the entrance hole of the deflector. A TV camera was placed in the yoke penetration originally designed for an injection current probe (θ=173°, fig. 1), and points towards the alumina plate through a mirror positioned close to one of the edges of the injection channel, so as not to stop the beam being injected.

Though the electric field value of the two deflectors necessary to extract the beam can be considered quite low for a machine commissioning, some problems of voltage holding arose mainly from the deflector E2. The entrance of E2 is in fact very close to one of the six accelerating gaps, and interaction with the RF system is supposed to be relevant. On the other hand, the gap between the electrode and

the septum was decided to be kept 8 mm wide according to the original design specifications, in order to avoid as much as possible beam losses inside the deflectors. However, since greater electric field values are required for future beams to be extracted, it is being planned to reduce the gap down to 6 mm.
The first magnetic channel (M1) is supposed to tilt a little bit (in the median plane), due to the position dependent field gradient. This has been ascertained several times after the magnet excitation at the end of the beam tests. A beam intensity loss is then expected because of the clearance reduction, so it is being planned to make the system more rigid.

7. Conclusion

Setting the extraction elements at the nominal values, a 0.5 enA beam was extracted on December 22nd 1994, the accelerated beam intensity being ~3 enA before E1. It is now planned to improve the extraction operation aiming to a better efficiency: since a strong dependance of the extraction parameters on the dee voltage has been ascertained, the knowledge of this parameter has to be acquired. Measurements based on the x-rays technique are planned for next future.
Even if the beam loss due to resonance crossing has not been so dramatic in the last tests, a proper centering detection and correction procedure has to be applied, since calculations do not take account of any off-centering. Some ideas are being developed about the use of the fixed centering probes which will be soon installed inside the machine.
An auxiliary TV camera is being planned to be installed inside the R.F. hole of one cavity to monitor the beam size directly at the stripper position so as to optimize the Tandem-Cyclotron matching.

8. References

[1] L. Calabretta et al., Towards the acceleration of the first beam by the INFN Superconducting Cyclotron, Proc. of EPAC 94, London, 1994, p. 551

[2] G. Cuttone et al., to be presented at XIV ICCA, Cape Town, 1995

[3] G. Raia, private communication

[4] L. Calabretta et al., Radial injection into the Superconducting Cyclotron at LNS, Proc. of EPAC 90, Nice, 1990, p. 1240

[5] G. Bellomo et al., The coupling line between the Tandem and the Superconducting Cyclotron at the LNS in Catania, Proc. of XI Int. Conf. on Cyclotrons and their Applications, Tokyo, 1986, p. 534

[6] K. Shima et al., Equilibrium charge fractions of ions of Z=4-92 emerging from a carbon foil, Atomic data and nuclear data tables 51, 1992,p.173, A.B. Wittkower et al., Equilibrium charge state distributions of energetic ions (Z>2) in gaseous and solid media, Atomic data 5, 1973, p.113

[7] G. Raia, private communication

[8] G. Bellomo, L. Serafini, Design of the magnetic field for the Milan Superconducting Cyclotron, Report INFN/TC-84/5, 1984

[9] P. Gmaj et al., Final mapping of the LNS Superconducting Cyclotron, Proc. of EPAC 94, London, 1994, p.2301

[10] G. Cuttone et al., to be presented at 2nd European Workshop on Beam Diagnostics and Instrumentation for Particle Accelerators, Travemunde, 1995

[11] E. Fabrici, A. Salomone, Acceleration studies for the Milan Superconducting Cyclotron, Report INFN/TC-83/9, 1983

[12] M.M. Gordon, Effects of spiral electric gaps in superconducting cyclotrons, N.I.M. 169, 1980, p. 327

[13] L.S. Milinkovic et al., Properties of centered accelerated equilibrium orbits, N.I.M. A273, 1988, p. 87

[14] E. Fabrici, A. Salomone, The extraction system for the Milan Superconducting Cyclotron, Report INFN/TC-87/4, 1987

[15] G. Cuttone, L. Calabretta, private communication

Captions

Tab. 1 Injection parameters

Tab. 2 Acceleration parameters

Tab. 3 Extraction parameters

Fig. 1 Median plane view of the Superconducting Cyclotron with the yoke penetrations

Fig. 2 Evolution of the horizontal beam ellipse along the injection path. The emittance value assumed is 4.8π mm·mrad.

Fig. 3 Horizontal and vertical envelopes of the beam along the injection trajectory.

Fig. 4 Use of the Cyclotron moving probe for the injection operation. The beam clears the stripper and is located on the moving probe at a radius of about 450 mm, quite different from the 150 mm injection radius.

Fig. 5 R - P_r plot at extraction. The beam ellipse is displayed once per turn at θ=100°, near the first deflector entrance.

Fig. 6 x - p_x plot for an off-centered beam.

Fig. 7 Beam vertical size for an off-centered beam in comparison to a centered beam.

Fig. 8 Effect of the extraction bump on the vertical size of an off-centered beam.

Fig. 9 Horizontal and vertical envelopes of the beam along the extraction path.

Tab. 1

V_{Tandem}	9.5 MV	σ_{11hor}	400.09 mm^2
Q_i	4	σ_{12hor}	- 188.88 mm mrad
Q_f	16	σ_{22hor}	89.23 $mrad^2$
$r_{stripper}$	14.5 cm	σ_{11ver}	57.80 mm^2
$\theta_{stripper}$	326.2^o	σ_{12ver}	-47.81 mm mrad
$B_{steer.magnet}$	2.171 kGauss	σ_{22ver}	39.93 $mrad^2$
R_{16}	78.95 mm/%	R_{26}	-39.16 mrad/%

Tab. 2

Q/A	0.276169923	I_α	1290.49 A
B_o	32.4224 kGauss	I_β	270.81 A
V_{dee}	50 kV	B_1	2 gauss
h	2	ϕ_1	60^o
f_{RF}	27.5 MHz	T/A	29.4 MeV/a.m.u.

Tab. 3

E_{E1}	74.398 kV/cm	r_{M3}	---
E_{E2}	74.398 kV/cm	r_{M4}	962.7 mm
r_{inE1}	864.6 mm	r_{M5}	996.4 mm
r_{inE2}	884.6 mm	r_{M6}	1021.9 mm
r_{M1}	910.5 mm	r_{M7}	1058.1 mm
r_{M2}	---		

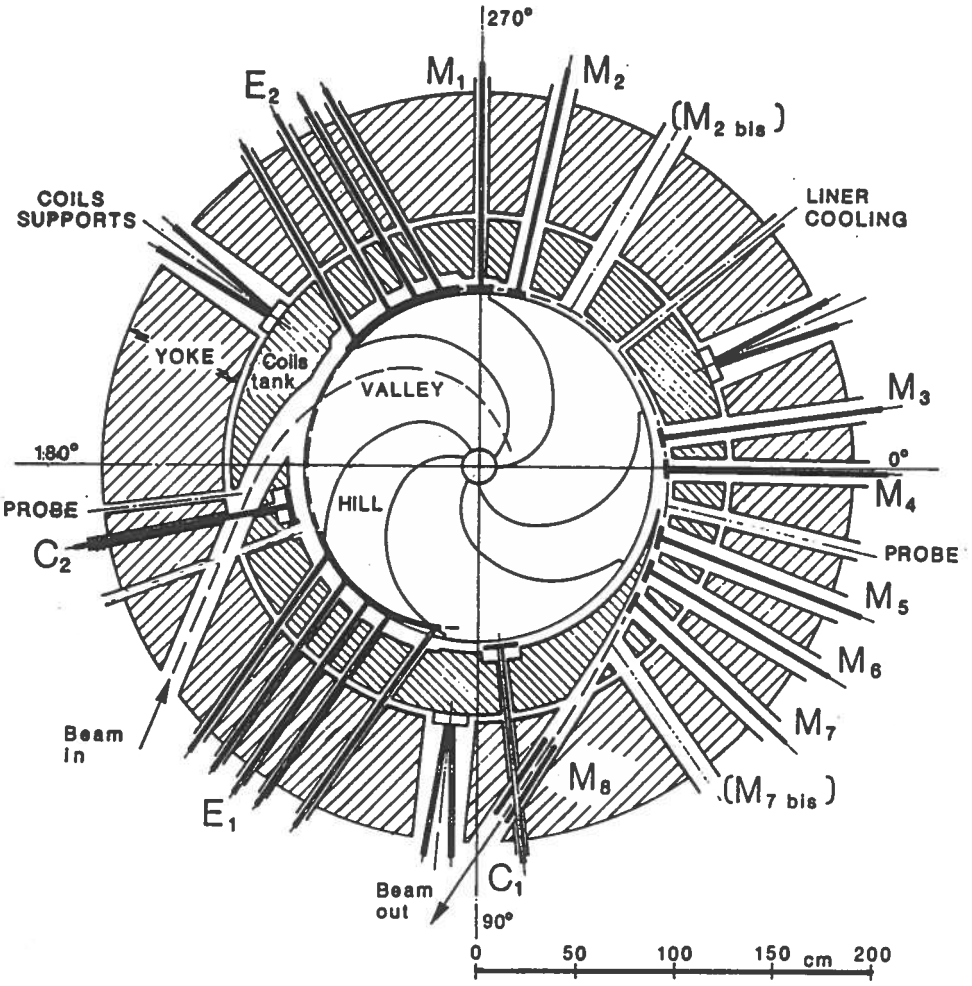
270°
E_2
M_1
M_2
($M_{2\ bis}$)
COILS SUPPORTS
LINER COOLING
YOKE
Coils tank
VALLEY
M_3
180°
0°
PROBE
HILL
M_4
PROBE
C_2
M_5
M_6
M_7
Beam In
M_8
($M_{7\ bis}$)
E_1
C_1
Beam out
90°
0 50 100 150 cm 200

Fig. 1

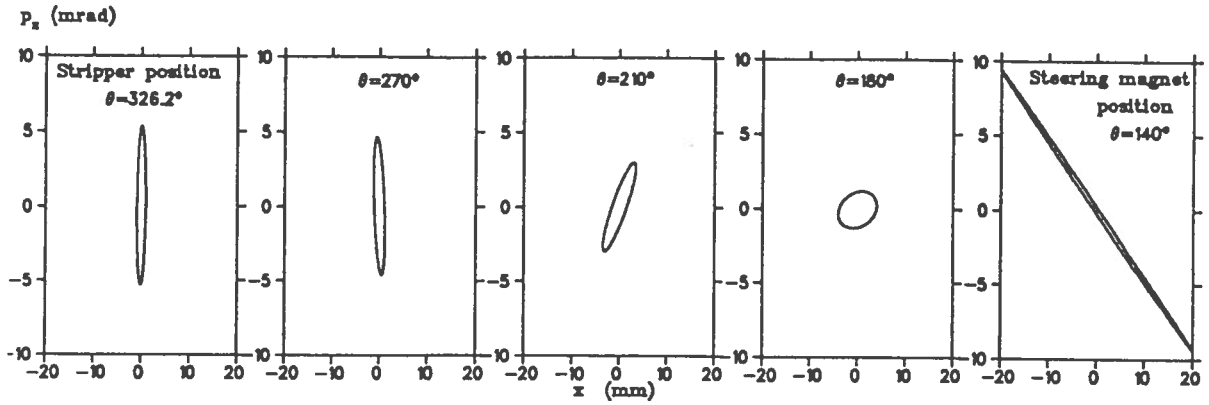
p_x (mrad)
Stripper position
θ=326.2°
θ=270°
θ=210°
θ=180°
Steering magnet
position
θ=140°
x (mm)

Fig. 2

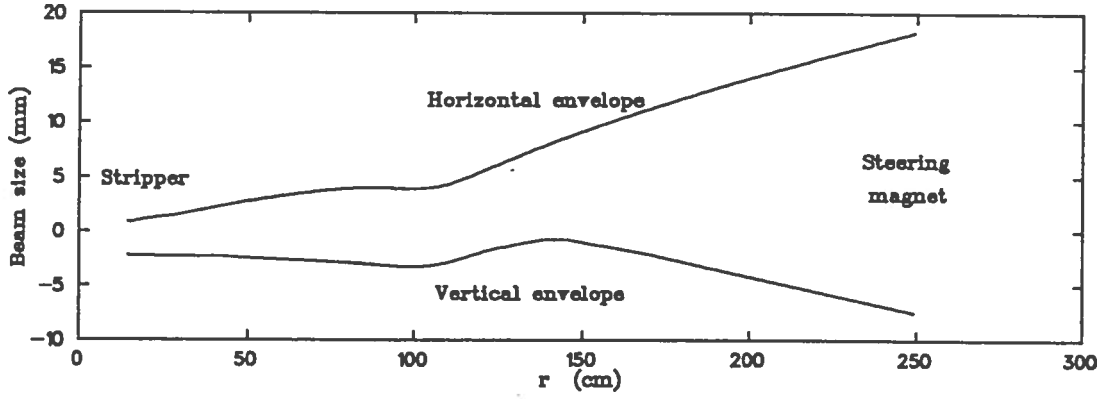
Beam size (mm)
Horizontal envelope
Stripper
Steering
magnet
Vertical envelope
r (cm)

Fig. 3

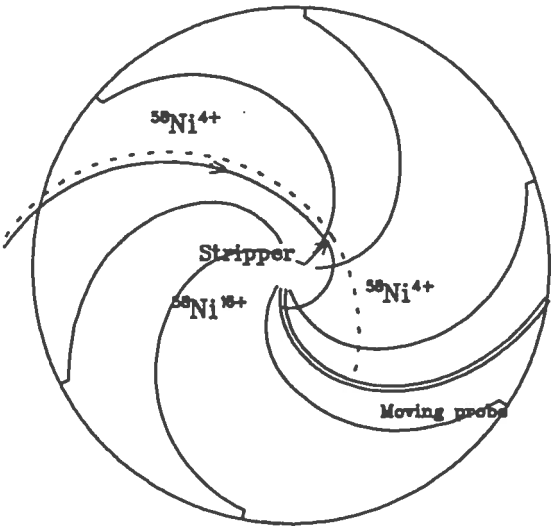
$^{58}Ni^{4+}$
Stripper
$^{58}Ni^{16+}$
$^{58}Ni^{4+}$
Moving probe

Fig. 4

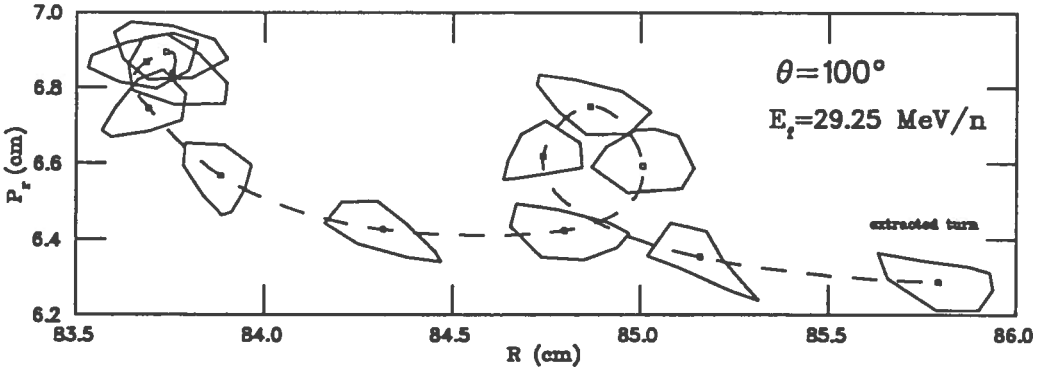
7.0
6.8
6.6
6.4
6.2
P_r (am)
83.5
84.0
84.5
85.0
85.5
86.0
R (cm)
θ=100°
E_i=29.25 MeV/n
extracted turn

Fig. 5

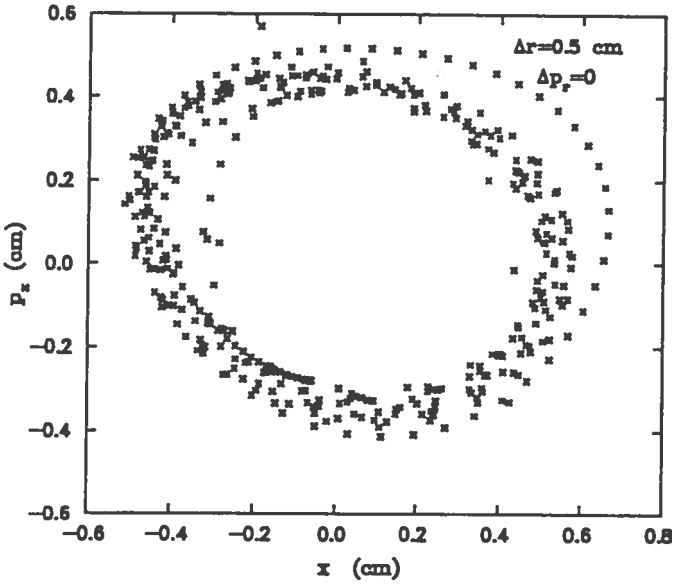
Δr=0.5 cm
Δp_x=0
p_x (cm)
x (cm)
0.6
0.4
0.2
0.0
−0.2
−0.4
−0.6
−0.6
−0.4
−0.2
0.0
0.2
0.4
0.6
0.8

Fig. 6

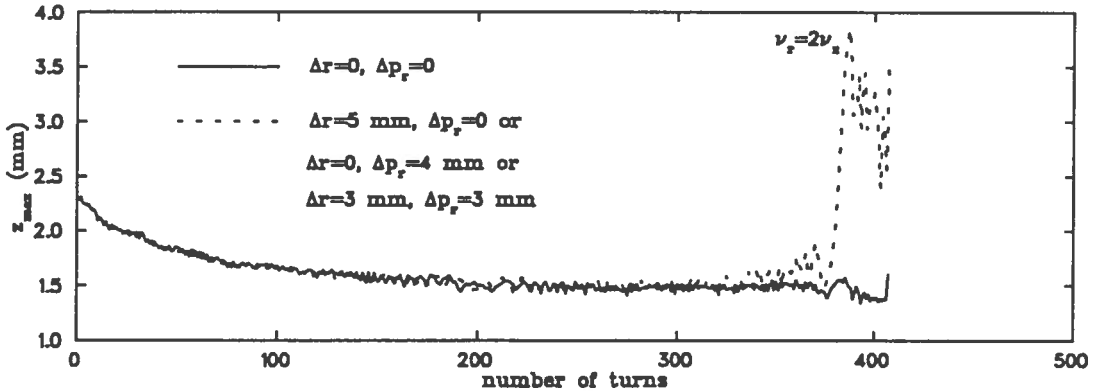
Δr=0, Δp_x=0
Δr=5 mm, Δp_x=0 or
Δr=0, Δp_x=4 mm or
Δr=3 mm, Δp_x=3 mm
ν_x=2ν_z
x_max (mm)
number of turns
4.0
3.5
3.0
2.5
2.0
1.5
1.0
0
100
200
300
400
500

Fig. 7

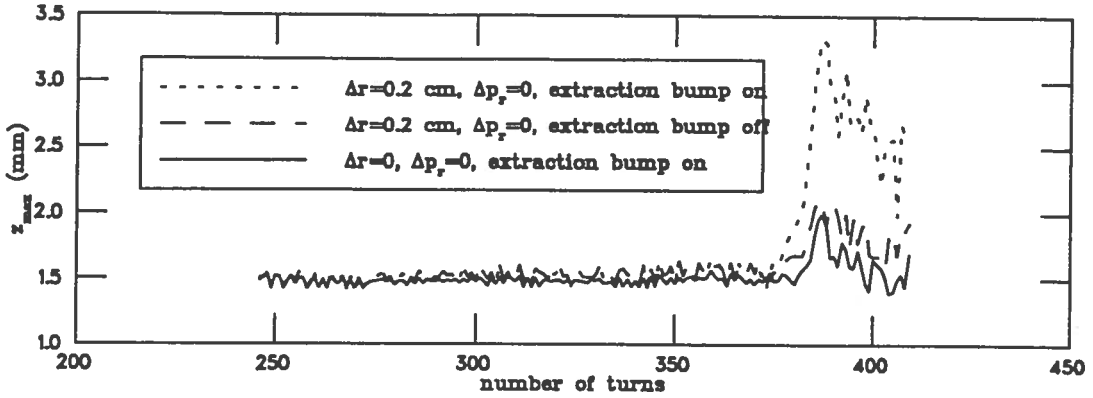
Δr=0.2 cm, Δp_r=0, extraction bump on
Δr=0.2 cm, Δp_r=0, extraction bump off
Δr=0, Δp_r=0, extraction bump on
x_max (mm)
number of turns

Fig. 8

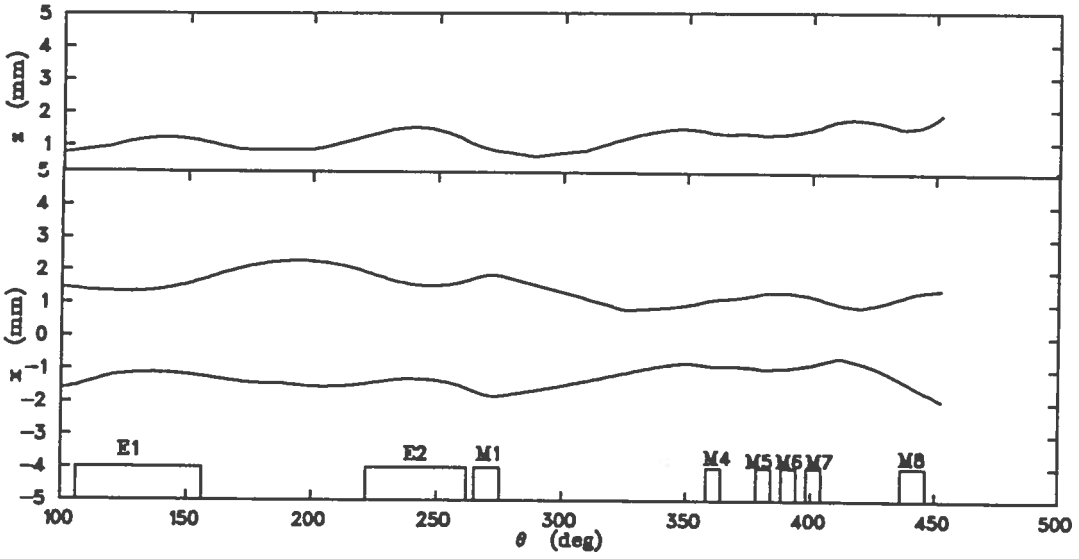
x (mm)
y (mm)
E1
E2
M1
M4
M5
M6
M7
M8
θ (deg)

Fig. 9